










Shape-Adaptive Universal Soft Parallel Gripper for Delicate Grasping Using a Stiffness-Variable Composite Structure

Jae-Young Lee , Yong-Sin Seo , Chanhun Park , Je-Sung Koh , *Member, IEEE*, Uikyum Kim , *Member, IEEE*, Jongwoo Park , Hugo Rodrigue , *Member, IEEE*, Byeungin Kim , and Sung-Hyuk Song 

Abstract—The robotic gripper is an essential component for handling, manipulating, and transporting objects. However, the parallel rigid gripper, which is one of the most widely used grippers in robotics, has limitations in handling fragile objects with a proper gripping force. We present a shape-adaptive universal soft gripper that can grip complex-shaped fragile objects with a high holding force. The shape-adaptive skin of the gripper has extremely low stiffness (~ 46 kPa), even lower than that of tofu (~ 57 kPa); hence, it can inherently prevent damage to the object. In addition, only the area pressed by the object is selectively deformed, so the contact surface of the gripper can be deformed to match the target object contour. A stiffness transition in the gripper from a soft to hard state follows to achieve effective holding of the object, not just weak object hanging as the previous soft gripper. These characteristics are enabled by a sheet-shaped shape retention layer, a honeycomb-shaped soft supporting layer, and a four-sided wall structure to increase shear modulus. We present applications to show the performance of the gripper, including gripping tofu, preparing a cocktail with a squeezed lemon, and whole chicken soup.

Index Terms—Shape-adaptive structure, soft robotics, stiffness-variable composite, universal parallel gripper.

Manuscript received June 26, 2020; revised October 5, 2020 and November 3, 2020; accepted November 25, 2020. Date of publication December 21, 2020; date of current version August 25, 2021. This work was supported by the National Research Council of Science and Technology (NST, Korea Government). (*Corresponding author: Sung-Hyuk Song.*)

Jae-Young Lee and Yong-Sin Seo are with the Department of Robotics and Mechatronics, Korea Institute of Machinery and Materials, Daejeon 34103, South Korea, and also with the School of Mechanical Engineering, Sungkyunkwan University, Suwon 16419, South Korea (e-mail: leejy@kimm.re.kr; sys7668@kimm.re.kr).

Chanhun Park, Uikyum Kim, Jongwoo Park, Byeungin Kim, and Sung-Hyuk Song are with the Department of Robotics and Mechatronics, Korea Institute of Machinery and Materials, Daejeon 34103, South Korea (e-mail: chpark@kimm.re.kr; uikykim@gmail.com; jekiel@kimm.re.kr; kimbil@kimm.re.kr; shsong@kimm.re.kr).

Je-Sung Koh is with the Department of Mechanical Engineering, Ajou University, Suwon 16499, South Korea (e-mail: jskoh@ajou.ac.kr).

Hugo Rodrigue is with the School of Mechanical Engineering, Sungkyunkwan University, Suwon 16419, South Korea (e-mail: rodrigue@skku.edu).

This article has supplementary material provided by the authors and color versions of one or more figures available at <https://doi.org/10.1109/TIE.2020.3044811>.

Digital Object Identifier 10.1109/TIE.2020.3044811

I. INTRODUCTION

AS THE usage of robots has extended beyond traditional manufacturing and industrial automation to the areas of service [1], medical [2], and human–robot collaboration [3], the need for an adequate end effector is increasingly important to accomplish these tasks. To perform various tasks, the end effector must be able to grip multiple types of target objects. The best option for handling target objects is a gripper with multiple fingers, similar to a human hand [4]; for this reason, several grippers have been researched and developed to achieve human-level object handling ability [5], [6]. However, as the number of actuating parts increases for dexterous motion, the hardware configuration becomes more complex, and the control of multiple actuators becomes more difficult, particularly when the shape of target object is irregular. Therefore, one of the most commonly used grippers in the industrial environment is the parallel gripper due to its structural simplicity [7]. Parallel grippers come in two types: force-fit gripping and form-fit gripping according to the tip shape [8]. Force-fit gripping uses the friction between the tips and the target object, so the compression force of each tip, which is usually named the gripping force, and the friction coefficient create the holding force. Therefore, the holding force is predetermined by the initial compression force. Conversely, form-fit gripping uses a specific shape tip tailored to the target object. The holding force in form-fit gripping is generally higher than that in force-fit gripping, but this advantage is only effective when the shape of the tip is matched to the target object [8], [9]. Therefore, a different type of tip must be employed whenever the target object is changed to realize effective gripping. In particular, we focus on universal form-fit gripping where the tip is passively modified to fit the shape of the target object so that efficient gripping without tip replacement can be achieved. In this case, the proposed universal parallel gripper can have the advantage of structural simplicity (as well as the platform’s popularity, which has been proven in the industrial field), representing a new type of gripper that can enhance the impact in industrial robots.

Methods for changing the shape of the gripper or tip using the stiffness transition mechanism for adaption to the target object have been studied previously, with the use of magnetorheological (MR), low melting point alloy, jamming mechanism using particles or layers. In the case of grippers that use MR fluid to change the stiffness, a magnetic field is applied to the fluid to increase the stiffness. The MR fluid is filled with a single

ball-shaped membrane [10], [11] or a ball-shaped flexible tip at a parallel gripper [12], [13]. However, the following limitations exist when changing the stiffness using MR fluid: hanging down of the ball-shaped structure owing to the large specific gravity and difficulties in increasing the stiffness significantly because of the rapidly decreasing magnetic flux density as the distance increases [11]. Therefore, it is difficult to construct a large gripper and changes in the stiffness cannot significantly affect the performance improvement. A stiffness transition using low melting point alloy has also been used in robot grippers [14]–[16]. However, the slow response time owing to the heating and cooling of the alloy to change the stiffness is a shortcoming of such an approach. Particle and layer jamming mechanisms are commonly used methods for changing the stiffness owing to their structural simplicity; stiffness changes occur as a result of pressure changes between the particles or layers [17]. John Amend developed the JamHand, which uses a ball-shaped membrane based on a particle jamming mechanism for a dexterous robotic hand [18]. This configuration is the same as that of the universal gripper that uses a ball-shaped rubber membrane [19], [20]. Particle jamming was also implemented in a finger-shaped gripper for shape adaptation to the target object and to increase the stiffness of the finger-shaped gripper [21], [22] and the particles for jamming were encapsulated in the form of a circular cylinder. Therefore, a sphere- or round-shaped structure is employed in most of these particle jamming grippers, which include a large volume of particles for shape adaptation because the jamming gripper is fully filled with granular material, and the compression force owing to the stretched enclosing membrane in the without-jamming state is equally distributed over the entire surface. This fully filled with granular material makes increase the initial stiffness of the gripper because a sequential material transfer corresponding to the volume of the target object is required. Therefore, this method exhibits a disadvantage in terms of shape adaptation for objects with low stiffness. As another method for changing the stiffness using jamming, layer jamming has been proposed, which uses the friction between the stacked layers. The layer jamming mechanism was applied in a gripper using vacuum [23], [24] or electrostatic force [25]. However, the majority of the developed layer jamming mechanisms were implemented only in the bending of rod-like structures or one-directional simple bending of plate-like structures, and could not be implemented for complex deformation in the plane. This is because the basic components constituting a layer jamming mechanism have a layer shape, so it is difficult to realize complex deformation forms.

In this research, we present a universal parallel gripper with a shape-adaptive tip to grip different types of objects of not only various shapes but also different degrees of stiffness. The shape-adaptive tip consists of a shape retention layer that can change the stiffness of the shape-adaptive tip and a soft supporting layer that helps the tip to be deformed according to the contour of the target object with low initial stiffness similar to the tofu. The shape retention layer is deformed by a sheet bending process instead of a volumetric transformation due to the soft supporting layer, which helps achieve a low initial stiffness of the gripping tip. Moreover, the structural configuration of the shape retention layer can increase the holding force through an up to 17.9 times difference in the tip shear modulus before and after the stiffness transition depending on the structural characteristics. Therefore, the key components of this gripper to have differentiated features from the previous studies can be summarized as follows:

- 1) a sheet-shaped shape retention layer capable of bending deformation and stiffness transition with a stretchable mesh structure;
- 2) a honeycomb-shaped soft supporting layer that minimizes deformation propagation due to its low surface tension;
- 3) a four-sided wall structure that increases the holding force due to the increased shear modulus.

The extremely low initial stiffness of the gripping tip, in addition to the high holding force, decreases the initial compression force required for a firm grip and enables various tasks involving fragile and/or vulnerable objects, such as tofu and grapes, as well as making cocktails by squeezing a lemon. This gripper can be used as a robotic harvesting system for bunches of grapes by direct firm grasping without damaging them [see Fig. 1(a)].

II. OVERALL DESIGN AND MECHANISM

The shape-adaptive soft composite gripper consists of two shape-adaptive tips in parallel, and the soft gripping tips are connected to parallel gripper (RH-P12-RN, Robotis). When the gripper tries to grab the target object, the two connected shape-adaptive tips in parallel are simultaneously actuated by the motor-driven 4-bar linkage mechanism. As the shape-adaptive tips become closer, the target object begins to make contact with the shape-adaptive tip surfaces, and the tip surfaces are deformed as each tip becomes closer. Both shape-adaptive tips are deformed by the shape of the target object at the point of contact. When the deformation of the shape-adaptive tips reaches the goal depth, the 4-bar linkage actuator stops the motion and maintains the distance between the tips. During this process, the shape-adaptive tips are soft enough, so the stiffness of the target object can be assumed to be generally higher than that of the tips. For this reason, the compression force required to close the two tips can be negligible in this ideal condition.

When the stiffness of the shape-adaptive tips is increased due to the shape retention layer, as shown in Fig. 1(b), the deformed shape of the tip that matches the shape of the target object is maintained in this manner. To increase the stiffness of the shape-adaptive tip, a negative pressure is applied in the component located inside the shape retention layer. After the deformed shape of the tip is fixed, the gripper begins to perform additional tasks, such as moving the object, during which an external force is applied to the tip due to the weight of the target object. External forces can be due to other types of tasks, such as inserting or joining operations. The direction of the external force is generally parallel to the contact surface of the shape-adaptive tip, so it generates shear stress at the tip, as shown in Fig. 1(c). In the figure, the shape retention layer, especially at the sidewall, is intended to be deformed from the rectangular shape to the parallelogram marked in green because of the shear stress. However, as a negative pressure is applied in the shape retention layer, the compressive forces among particles are increased. This creates increased frictional forces among the particles, especially in the shear direction, as shown on the right side of Fig. 1(c), indicating that the shear modulus is dramatically increased. The bending stiffness does not significantly differ before and after the negative pressure is applied in this configuration because the tensile force accompanied by the bending operation mainly affects the membrane, not the particles themselves in this shell-like structure. Therefore, a high shear

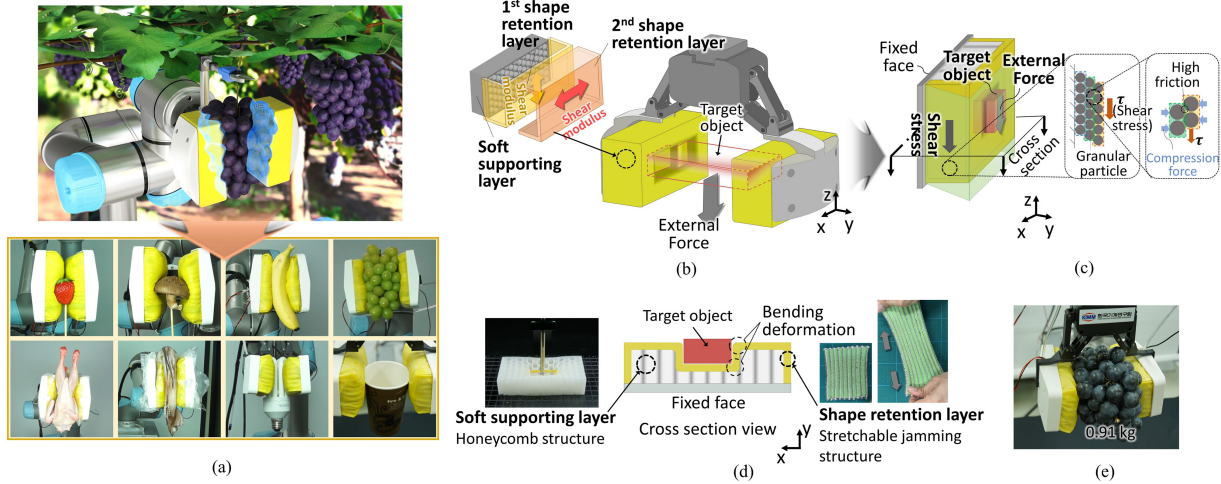


Fig. 1. Configuration of the shape-adaptive composite gripper. (a) Illustration of an example application of the soft gripper for harvesting a bunch of grapes. (b) Schematic view showing the components of the shape-adaptive universal soft parallel gripper. (c) Stiffness transition mechanism in the shear direction due to the vacuum shape retention layer. (d) Detailed configuration of the shape-adaptive tip consisting of a soft supporting layer and a shape retention layer. (e) Image of the developed gripper holding a bunch of grapes weighing 0.91 kg without damaging the grapes.

modulus of the shape retention layer can only be achieved when the direction of the applied external force is parallel to the plane of the sidewall of the shape retention layer. Because of this, two different configurations of shape retention layers are embedded, as shown on the left side of Fig. 1(b). A more detailed experiment was performed and is described in the following section.

Through these processes, the shape-adaptive composite gripper can handle the target object. The main advantage of the developed gripper is the large holding force in the stable gripping state, with a low initial compression force due to the extremely soft state of the gripping tip. To achieve this unique advantage, two main elements are combined in a composite made of a soft supporting layer and a shape retention layer, as shown at Fig. 1(d). The soft supporting layer helps deform the tip so that they match the contour of the target object as much as possible. The closer the deformed shape of the tip is to the shape of the target object, the more stable the grip that can be achieved. The shape retention layer also helps the tip deform to the shape of the target object due to its stretchable structure. The other goal of these two elements is to decrease the initial tip stiffness. The shape retention layer consists of a shell-like shape, so the bending deformation becomes dominant while the target object pushes against the surface. The bending deformation requires a much smaller force than the volumetric deformation that occurs when bags are fully filled with particles, as described earlier. The combination of these factors makes it possible to hold an extremely soft object regardless of its shape, such as a bunch of grapes, as shown in Fig. 1(e).

A. Design of the Soft Supporting Layer

As described in the previous section, the soft supporting layer consisting of a honeycomb structure plays a vital role in deforming the tip surface to match the shape of the target object. The shape of deformed soft supporting layer due to the target object can be described using the Filonenko–Borodich model, which uses the individual spring elements in the Winkler model and the elastic membrane connecting the spring element under a constant tension T [26], [27]. The surface deformation w of the

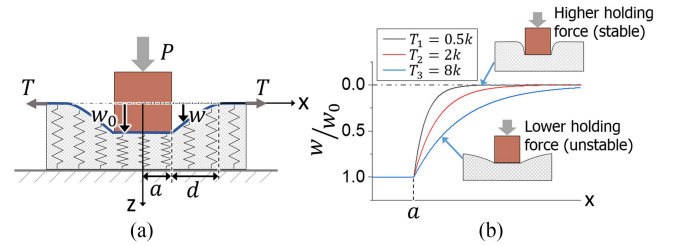


Fig. 2. Theoretical model of the soft supporting layer. (a) Definition of parameters to represent the effect of surface tension on the deformation shape of the soft supporting layer. (b) Shape of surface deformation depend on the surface tension.

structure due to a pressure q in the elastic half space is described as follows:

$$q(x, y) = kw(x, y) - T\nabla^2 w(x, y) \quad (1)$$

where the k is the spring constant, which is relative to the modulus of structure without the influence of surface tension. In the two-dimensional approximation, equation can be reduced to

$$q(x) = kw(x) - T\frac{d^2 w(x)}{dx^2} \quad (2)$$

as described in Fig. 2(a). If the applied pressure due to the target object is assumed as constant p at the contact area between the structure and the target object, the force F_z at membrane when $x \geq 0$ is

$$\Sigma F_z = \int_0^\infty (q(x) - kx(x))dx = \frac{P}{2} - k \int_0^\infty w(x)dx = 0 \quad (3)$$

where

$$P = \int_{-\infty}^\infty q(x)dx = 2pa. \quad (4)$$

Therefore, the surface deformation is calculated as follows:

$$w(x) = \begin{cases} w_0, & \text{for } x \leq a \\ w_0 e^{-r(x-a)}, & \text{for } x > a \end{cases} \quad (5)$$

where

$$r = \sqrt{\frac{k}{T}}, \quad w_0 = \frac{rP}{2k}. \quad (6)$$

The shape of surface deformation depends on the surface tension as described in Fig. 2(b). As the surface tension decreases, the ratio of surface deformation w to the maximum deformation distance w_0 shows rapidly decreases. It means that the distance of deformation propagation d in Fig. 2(a) decreases and the deformation of the structure can be matched to the target object. Then, the target object can be firmly and stably held—buried in the supporting layer—as the deformed supporting layer surrounds the target object. In respect with the force required to make deformation, the compression force P can be explained as the following equation:

$$\begin{aligned} \frac{P}{2} &= \frac{1}{2} \Sigma F_{\text{spring}} = k \int_0^{\infty} w(x) dx \\ &= k \int_0^a w(x) dx + k \int_a^{\infty} w(x) dx \\ &= \frac{P_0}{2} + \frac{kw_0}{r} \end{aligned} \quad (7)$$

where

$$P_0 = kw_0 a. \quad (8)$$

Therefore, the required force P becomes P_0 as the surface tension approaches 0, however, the required force increases as the surface tension increases. It means that the reaction force transferred to the target object due to the deformation of shape-adaptive tip can be minimized and it can prevent damage on the target object when the surface tension is minimized.

In this respect, the honeycomb structure can be a good solution due to its low surface tension because hexagonal holes are formed vertical to the surface that the target object pushes against. These holes maximize the surface elongation and prevent deformation propagation along the surface. As shown in Fig. 3(a), the soft supporting layer is deformed as the indenter tip gradually descends, but the deformation is only concentrated at the position below the indenter. This unique characteristic of the honeycomb structure is clearly shown in Fig. 3(b). Even though the different structures on the left and right sides of the figure have the same dimensions, the value of d , the distance in which the deformation propagates along the surface, is much smaller for the honeycomb structure than for the sponge block. The details of the honeycomb structure under deformation are shown in Fig. 3(c). The original hexagonal geometry before the deformation is marked in green. After the indenter is pushed into the honeycomb structure, the hexagonal cell located near the indenter is elongated from the shape marked in red to the shape marked in purple. However, the deformation is not propagated to the next hexagonal cell, marked in blue, because the adjacent hexagonal cell retains its original shape, whereas the elongated cell absorbs the impact of the deformation due to the hole

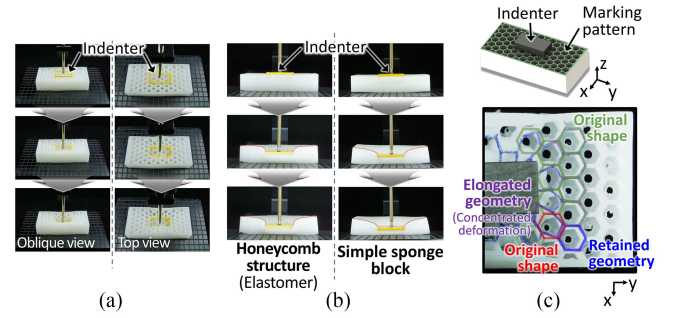


Fig. 3. Characteristics of the soft supporting layer. (a) Image of a soft supporting layer pressed with a transparent indenter tip. (b) Comparison of deformed shapes in a side view between the honeycomb structure and a simple sponge block. (c) Image of deformation of the soft supporting layer due to the indenter showing how the honeycomb structure prevents the propagation of deformation.

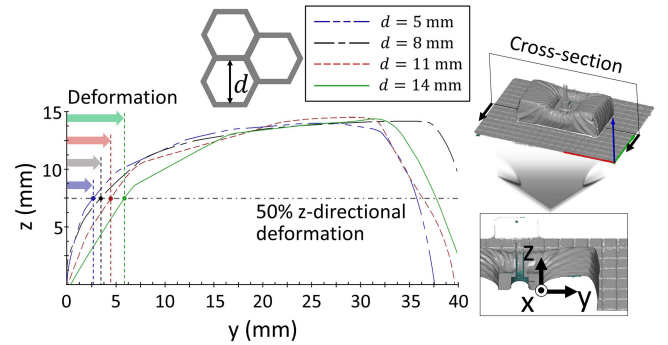


Fig. 4. Contours of cross-sectioned honeycomb structure depending on hole size when indenter tip is pushed downward.

penetration along the height. Therefore, the initial force required to deform the shape-adaptive tip to match the target object can be minimized, along with the tip deformation that exactly matches the shape of the object as described in Fig. 2.

Such an effect is difficult to achieve when only multiple circular penetrating holes exist. Because the hole size needs to be large enough to minimize the surface tension, the wall thickness cannot be uniform along the surface. In the case of a triangular or a rectangular pattern, the increased nonhomogeneity of the wall stiffness due to the increased influence from the vertices is disadvantageous; moreover, these structures are not as effective in supporting the shape retention layer after the jamming transition due to stress concentration at the vertices.

To evaluate the propagation distance according to the size of honeycomb structure, the deformed surface shape was measured using a cross-section of the measured three-dimensional data, as depicted in the right side of Fig. 4. Then, the contour of the cross-section was analyzed with respect to the distance from the edge of the indenter tip and the height of the honeycomb structure. To compare how the tip was deformed to fit the target object and the magnitude of the deformation propagation distance depends on the honeycomb hole size d , the distance from the edge of the indenter tip where the structure was deformed to 50% of the total depth of deformation in the z -direction was measured. As can be observed from Fig. 4, the honeycomb structure with an 8 mm size exhibited the shortest distance

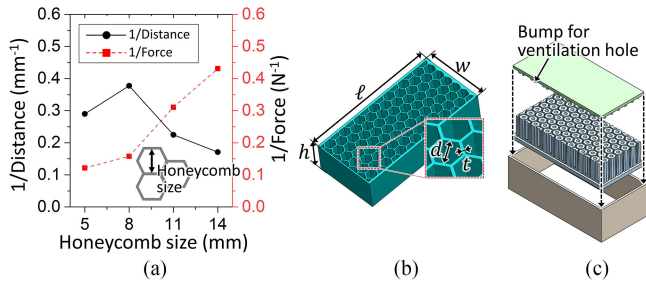


Fig. 5. Characteristics of soft supporting layer. (a) Deformation distance and stiffness of honeycomb structure depends on the hole size. (b) Illustration of dimensions of honeycomb structure in soft supporting layer. (c) Casting mold components and direction of assembly process to fabricate soft supporting layer.

among the honeycomb sizes; thus, the 8 mm size honeycomb could be deformed the most to match the target object. In the case of a 5 mm honeycomb size, the deformation distance was the shortest near the indenter, but it increased as the distance from the indenter increased. As the honeycomb size increased, the deformation distance also increased when the honeycomb size was larger than 8 mm. This is because if the honeycomb hole size is too large, the gap between the walls in the honeycomb will be too large, making it difficult to prevent deformation propagation in the wall-to-wall space. On the other hand, if the honeycomb hole size is too small, the characteristics of the structure become similar to those of a homogenous structure, and it is difficult to achieve the effect of surface tension minimization using the holes, as described earlier. Another aspect to consider for the appropriate hole size of the honeycomb structure is the stiffness of the structure because the possibility of object damage owing to the compression force can be minimized as the stiffness of the structure decreases. The reaction force of the indenter tip was measured when the indenter tip was pushed to a depth of 15 mm, which was the maximum target compression depth. As the honeycomb hole size increased, the reaction force decreased. The data obtained when considering the deformation distance and stiffness simultaneously are presented in Fig. 5(a). In this experiment, a honeycomb structure with a hole size of 8 mm was selected because this size exhibited the best performance in the shape-fitting deformation and a relatively lower stiffness. To fabricate a softer gripper for gripping more fragile objects, a honeycomb with a larger size could be selected. The dimensions and detailed shape of the honeycomb structure used as the soft supporting layer are illustrated in Fig. 5(b). The length l was 115 mm, the width w was 56 mm, the height h was 27 mm, the honeycomb hole size d was 8 mm, and the honeycomb wall thickness t was 1 mm. To fabricate the honeycomb structure, three components were used as a casting mold, as illustrated in Fig. 5(c). The uppermost part of Fig. 5(c) is the cover to limit the height of the cured structure, which had small bumps to form ventilation holes through the honeycomb structure. The size of the casted ventilation holes was 3 mm, which aided in ventilating the air trapped inside the honeycomb structure when the object was pushed against the surface. After assembling the two lower parts, Ecoflex-0020 polymer (Smooth-On) was poured into the empty space and covered the uppermost part of the casting mold component. The polymer was cured at room temperature for one day, following which the honeycomb structure was demolded from the casting mold.

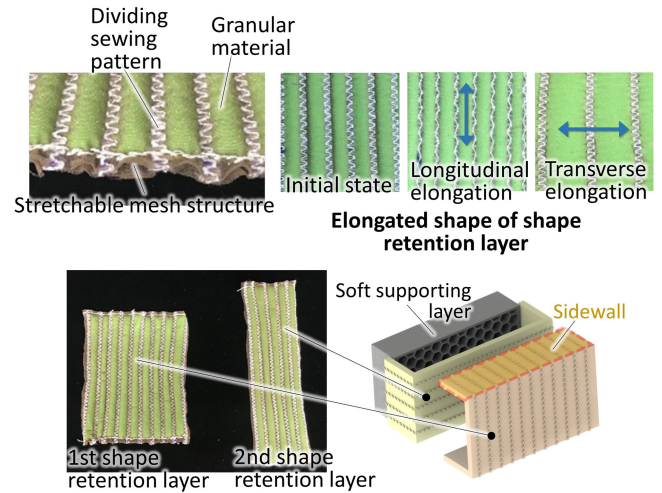


Fig. 6. Configuration of the shape retention layer with a stretchable mesh structure and granular particles.

B. Design of the Shape Retention Layer

To retain the deformed shape fitted to the shape of the target object, a shape retention layer is required. The surface tension of the shape retention layer also needs to be minimized using low modulus structures in the tensile direction, as described in a previous section. Therefore, the shape retention layer is fabricated using a highly stretchable mesh structure. The 30 denier stocking fabric was used as the stretchable mesh structure due to its high stretchability and durability. Inside the mesh structure, a granular material is filled in a sheet shape. The granular material used was pulverized sand and its average size was approximately $250 \mu\text{m}$. Sewing is applied to the stretchable mesh structure to divide the space and maintain the position of the granular material during operation. A zigzag sewing pattern is used, as shown in Fig. 6; it can be stretchable not only in the vertical direction of the sewing line but also in the horizontal direction. The stretchable mesh structure is encapsulated by a stretchable elastomer membrane to create a vacuum environment. The 0.16 mm thick rubber sheet (TheraBand) was used as the stretchable elastomer membrane. Two different stretchable mesh structures are layered vertically according to the sewing direction because the locations where the granular particle is not filled, due to the sewing pattern positioning, can be covered by the adjacent mesh structure positioned vertically, and the shape retention layer can be achieved by increasing the stiffness in all directions after the jamming process. The sizes of the stretchable mesh structures were 170 mm (length), 56 mm (width), and 5 mm (thickness); and 120 mm (length), 120 mm (width), and 5 mm (thickness).

The detailed process of how the target object is held is depicted in Fig. 7. First, the target object is pushed toward the tip while the gripper is closing; then, the tip starts to make contact with the target object (1st step in Fig. 7). At this point, the shape retention layer is in a soft state, and the force is concentrated only under the area where the target object is located due to the low surface tension (second step). The gripper continues to close, moving the tip until the soft supporting layer deforms to the target depth (third step). During this process, the shape retention layer deforms via bending, so the force required for

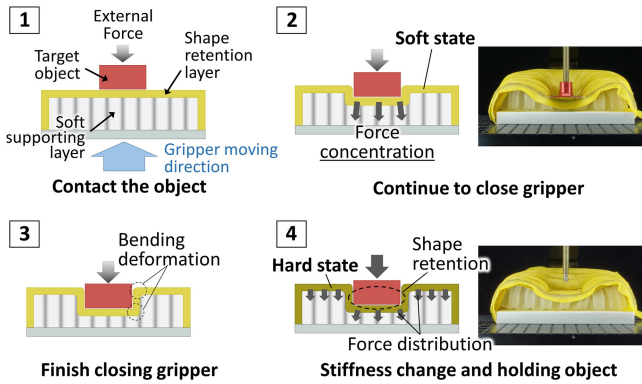


Fig. 7. Sequence of holding target object in the shape-adaptive tip.

deformation can be minimized. The modulus of tip in soft state was measured as 80.17 kPa at first modulus region and 46.39 kPa at second modulus region. The second modulus region of tip was even lower than the modulus of tofu, which is ~ 57 kPa. After the target depth is reached, the shape retention layer is changed to a hard state using the jamming process (fourth step). In this state, the deformed shape of the shape retention layer is maintained, as shown in the right side picture of Fig. 7, and the whole shape retention layer acts as a single rigid structure maintaining the deformed shape of the soft layer (Supplementary video 1). If additional external forces arise from the target object weight or from performing a specific task, they can be distributed over the entire surface of the shape retention layer, and the distributed force can be supported by the whole soft supporting layer area. This can be explained by the increased surface tension of the shape retention layer after jamming, as it can effectively withstand the additional forces.

After the task is finished, the vacuum environment of the shape retention layer is changed to normal atmospheric pressure, and the hard state changes to the soft state. Then, the gripper retracts the tip. The target object is then released from the gripper, and the deformed shape of the shape retention layer returns to the original shape because of the elastic restoration of the soft supporting layer.

To effectively hold the target object during transfer, the shear stress in the tip is critical, as illustrated in Fig. 1(c). The role of the sidewall of the shape retention layer is to endure the additional external force in the shear direction during the task. However, a shear force applied normal to the sidewall of the shape retention layer cannot be properly supported, as shown for orientation #2 of Fig. 8(a). To compare how effectively the structure can support a shear force, an experimental setup was created, as shown on the left side of Fig. 8(a), to measure the shear modulus of the shape retention layer. Orientation #1 shows a modulus 4.4 times that in orientation #2 in the without-jamming condition, and this difference becomes much higher (17.9 times) in the jamming condition. The results prove that orientation #1 is more effective in enduring external forces. The shape retention layer can effectively endure external forces in both directions by arranging two different direction layers.

To achieve a stable and effective grip, the tip must be deformed to match the contour of the target object, as described in the previous section. As shown in Fig. 9 for the following

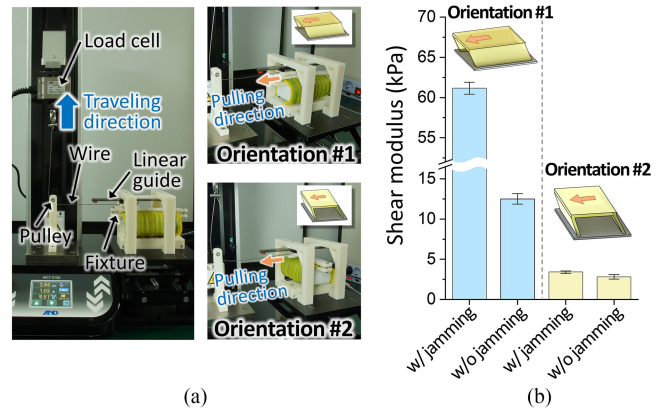


Fig. 8. Shear modulus of the shape retention layer depending on the orientation. (a) Experimental setup. (b) Measured shear modulus depends on the orientation.

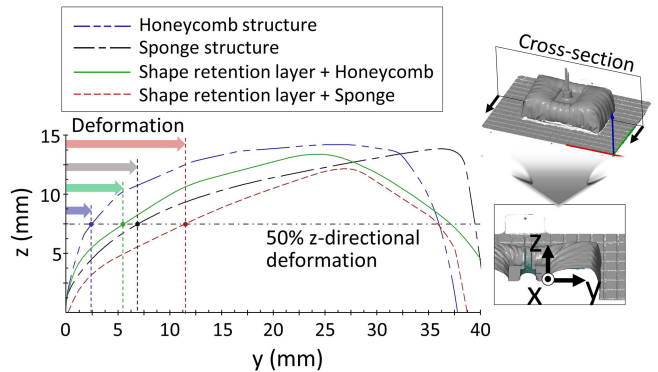


Fig. 9. Contours of cross-sectioned structures of sponge, soft supporting layer, and shape retention layer with honeycomb and sponge structures when indenter tip is pushed downward.

four different cases: a general sponge, a soft supporting layer only, sponge structure with a shape retention layer, and a soft supporting layer with a shape retention layer, which is the proposed composition of the tip. The honeycomb structure shows a 2.4 mm distance to 50% of the total depth of deformation, and this structure can be said to have a low surface tension and to be mostly deformed to match the target object. In contrast, the general sponge structure covered with a stretchable membrane shows a 6.8 mm distance, which is 2.8 times the distance with the honeycomb structure. When the honeycomb structure is combined with the shape retention layer, it shows a longer distance than the honeycomb-only structure but a shorter distance than the general sponge structure. The simple sponge structure combined with the shape retention layer had a 11.5 mm deformation distance, which was approximately 2.1 times larger than the honeycomb structure with the shape retention layer. This is because the deformation distance increased further when the shape retention layer was combined with the sponge structure, which already had a relatively large deformation distance. The other advantage of the honeycomb structure as a soft supporting layer is the small force required to deform it as described previous section, and this value does not change much even when the deformation magnitude increases. As indicated in Fig. 10,

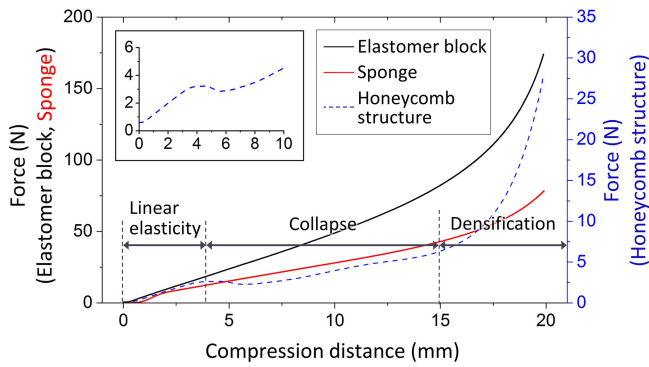


Fig. 10. Force required to cause deformation versus the compression distance for the elastomer block, sponge, and honeycomb structure.

the force required for deformation was compared for the bulk block-shaped structure, sponge, and honeycomb structure. The bulk block-shaped and honeycomb structures were fabricated using the same material, which had an extremely low modulus, with a Shore 00 hardness of 20. As expected, the elastomer block was confirmed to show a much higher modulus than the honeycomb structure, and the trends of the changes in the modulus were compared using different scales for the y -axis. In the case of the elastomer block, the force linearly increases as the compression distance increases in the initial deformation zone. However, the force required for deformation exponentially increases when the deformation depth reaches 15 mm or more. This trend was similarly demonstrated in the sponge structure, but it had a relatively lower stiffness than the elastomer block. In contrast, in the case of the honeycomb structure, the required force decreases as the deformation increases after the initial linear region, and then, the force slowly increases up to an approximately 15 mm depth. This zone can be classified as the collapse zone, which is followed by an initially linear elasticity zone. This result occurs because the honeycomb structure is linearly deformed at the beginning of the force application, but the honeycomb structure starts to collapse after the threshold point of the applied force is reached. As the collapse finishes, the collapsed structure starts to densify into a bulk structure, and the required force then starts to exponentially increase, similar to the elastomer block. Therefore, the tip can be effectively deformed with a small compression force if the deformation is less than 15 mm, which is the end of the collapse region. Furthermore, in this region, the required force is not greatly increased even when the magnitude of deformation is increased; the gripper does not need to control the gripping force during the closing of the tip regardless of the closing distance or the deformation magnitude. In contrast, if the elastomer block is used as the supporting layer in the tip, then the force required to close the gripper tip would dramatically change, as it depends on the closing distance and the deformation magnitude, and the gripper should limit the closing distance when the target object is fragile and/or easily damaged.

III. PERFORMANCE EVALUATION

The performance of the developed gripper was evaluated by measuring the holding force versus normal force. The normal force is defined as the initial compression force applied by the

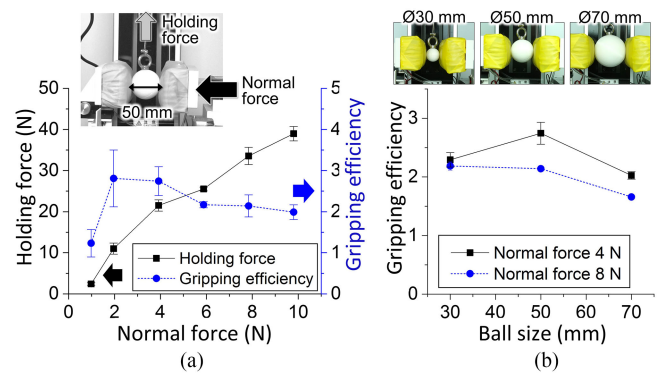


Fig. 11. Evaluation of the basic gripping performance. (a) Holding force and gripping efficiency versus the normal force when the target object has a $\phi 50$ ball shape. (b) Variation in the gripping efficiency with the size of the target object.

gripper tips to the target object. This force was measured by a load cell installed directly behind one of the gripper tips. The holding force is defined as how well the gripper can hold the object, and it was measured as the maximum force of a tensile machine when the object was pulled. For the general force-fit parallel gripper, the holding force is determined by the normal force because the holding force is mainly generated from the friction force. Therefore, the normal force must be increased to increase the holding force. Additionally, a high holding force in conjunction with a small normal force can be defined as an effective gripping condition in terms of low possibility of damage to the target object while maintaining an effective grip. Based on this, the gripping efficiency is defined as follows:

$$\text{Gripping efficiency} = \frac{\text{Holding force}}{2 \text{ Normal force}}. \quad (9)$$

The normal force in the denominator term is multiplied by a factor of two because the applied normal force is measured on one side, and we also need to consider the effects of the action/reaction law. This gripping efficiency can be defined as the friction coefficient for the normal force-fit parallel gripper with two tips.

Fig. 11(a) shows that the holding force and gripping efficiency depend on the normal force when the target object is a 50-mm diameter ball. As the normal force increases, the holding force also increases, similar to the force-fit gripper. However, the gripping efficiency values show much better performance than that for the usual force-fit gripper. This improvement is due to the tip's ability to adapt to the contour of the target object along with the tip changing to the hard state from the soft state, similar to the form-fit-based parallel gripper with the tip that has the same surface shape as the object. The difference between the traditional form-fit-based gripper and the developed shape-adaptive soft gripper is that the soft gripper cannot maintain its shape when an external force is applied that exceeds the threshold force. The threshold force to hold the target object can be defined as 11.0 N when the normal force is 2 N, and the gripper cannot hold the target object if the external force exceeds 11.0 N for this condition. As the normal force increases, the deformation magnitude also increases, and the tip better adapts to the target object. Then, the threshold force for holding the object also increases up to 38.9 N when the normal force is 10 N.

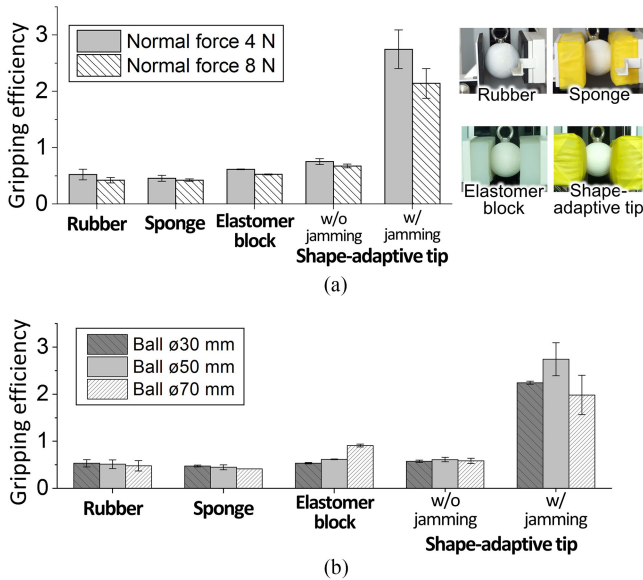


Fig. 12. Gripping efficiency test for five different tips. (a) Gripping efficiency depends on normal force. (b) Gripping efficiency with the size of target object.

The highest gripping efficiency was measured when the normal force was 2 N, and the gripping efficiency gradually decreases as the normal force increases. Therefore, the threshold force to maintain the deformed shape of the tip can be assumed to become most efficient when the normal force is 2 N because of the increased stiffness and not because of the influence from the friction force or other force factors that increase as the normal force increases.

To verify the effect of the size of the target object, the gripping efficiency was measured for three different ball sizes, as shown in Fig. 11(b). In all cases, a 4 N normal force shows a higher gripping efficiency than an 8 N normal force, and the gripping efficiency is the lowest when the ball size is the largest. The effect due to the size is because the depth of deformation decreases as the contact area between the target object and the tip increases for the same normal force, and the depth of deformation is related to how matched the tip is to the target object. The high gripping efficiency of the shape-adaptive tip could be assumed to be achievable without stiffness transition, so the effect of the stiffness transition using the jamming mechanism was verified, as shown in Fig. 12(a). The following five different types of tips were used: a rubber tip, a sponge tip, elastomer block, and the developed shape-adaptive tip with/without jamming. The rubber tip represents the normal force-fit parallel gripper, which usually uses a rubber tip to increase the friction coefficient. The sponge tip represents a soft state of the tip, so it can be deformed when a normal force is applied but does not adapt its contour as much as the shape-adaptive tip. The elastomer block also can be deformed due to its elasticity, but the deformation depth of the elastomer block is smaller than that of the sponge tip due to its high hardness. The rubber, sponge, elastomer block, and shape-adaptive tips without jamming exhibit gripping efficiencies in the range typical for a force-fit gripper, which vary from 0.2 to 0.4 for a general gripper [28], [29] and 0.36–0.64 for a sponge gripper [30]. However, the average gripping efficiency

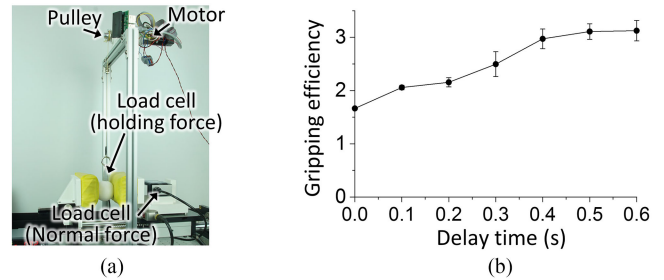


Fig. 13. Required time to switch stiffness. (a) Experimental setup. (b) Gripping efficiency depends on the delay time of pulling out object.

of the shape-adaptive tip with the jamming state is 4.51 times those in the other cases, which demonstrates that the stiffness transition is key for achieving a high gripping efficiency.

This trend was maintained even when the size of the target object was changed, as shown in Fig. 12(b), and the change in the object size did not significantly affect the gripping efficiency for the rubber tip, sponge tip, and shape-adaptive tip without jamming, unlike for the shape-adaptive tip with the jamming state and elastomer block. This occurs because these three control groups (rubber tip, sponge tip and shape-adaptive tip without jamming) cannot use the form-fit gripping-like effect because the rubber tip cannot be deformed and the sponge tip and shape-adaptive tip without the jamming state cannot maintain the shape, so the friction force, which is not affected by the size of the target object, becomes the dominant parameter for achieving the holding force. In case of elastomer block, the contact surface between the ball and elastomer block increases as the size of ball increases, then the gripping efficiency increases. This is because the area of elastomer block that is in contact with the ball can support effectively due to its relatively high hardness compared to the sponge and shape-adaptive tip without jamming.

The time required to switch the stiffness for effective high gripping efficiency was measured (see Fig. 13). Unlike in the previous experimental configuration, the system was controlled using a motor, as indicated in Fig. 13(a). This is because the object needed to be pulled at a high speed, with a synchronized starting time of the operation of the motor and vacuum pump. The gripping efficiency was measured by changing the starting time of pulling the object from the gripper after the vacuum pump was turned ON. It can be observed that the gripping efficiency converged from approximately 0.4 s after the pump started to operate.

Fig. 14 shows the gripping efficiencies for various objects with different shapes measured, and the dimensions of the objects are described in Fig. 15. Standard target object shapes, such as a cylinder, a cube, a cuboid, and a sphere, were tested. The results show that when the contact surface of the target object is flat, such as with the cube and the cuboid, the gripping efficiency is relatively low regardless of the size of the object. This is because the flat contact area equally distributes the compression force over the contact area, so the depth of deformation is relatively low when the total normal force is kept constant. In contrast, when the contact surface has a curvature or an irregular shape, the compression force can be concentrated in certain areas, and the depth of deformation increases; then, the gripping efficiency can be improved.

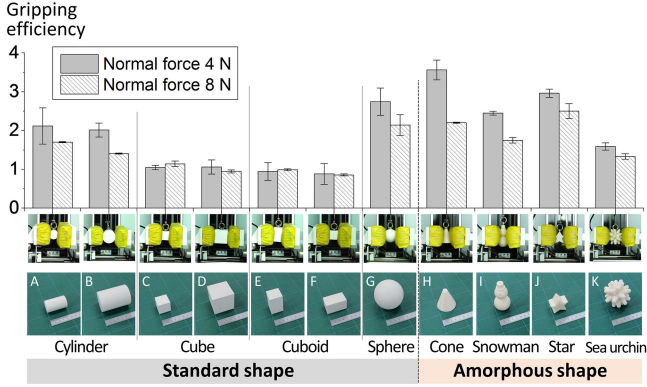


Fig. 14. Gripping efficiency measurements depending on the shape of the target object.

Object shape	No.	Dimension	Object shape	No.	Dimension	Object shape	No.	Dimension
	A	$R : 30 \text{ mm}$ $h : 50 \text{ mm}$		G	$R : 50 \text{ mm}$		J	$\theta : 38^\circ$ $h : 40 \text{ mm}$
	B	$R : 50 \text{ mm}$ $h : 70 \text{ mm}$						
	C	$a : 30 \text{ mm}$		H	$R : 25 \text{ mm}$ $R' : 5 \text{ mm}$ $h : 50 \text{ mm}$		K	$a : 4 \text{ mm}$ $h : 17 \text{ mm}$
	D	$a : 50 \text{ mm}$						
	E	$a, b : 30 \text{ mm}$ $h : 50 \text{ mm}$		I	$R : 20 \text{ mm}$ $R' : 15 \text{ mm}$ $h : 77 \text{ mm}$			
	F	$a : 50 \text{ mm}$ $b, h : 30 \text{ mm}$						

Fig. 15. Shape and dimension of various target object.

IV. PRACTICAL APPLICATION

To evaluate the performance of the gripper in more diverse circumstances, tasks that are difficult to perform with a normal gripper were identified and tested, as shown in Fig. 16. The target objects used in the evaluation were extremely soft but had a certain weight, such as a ripe persimmon, a tomato, and even tofu, or they had extremely irregular shapes, such as a bunch of grapes. In this case, the contact surface between the grapes and the tips had to be very tight to be able to adequately distribute the stress and hold the grapes; otherwise, the grapes would be easily damaged or be dropped. Fig. 16(e) shows that the gripper can pick up the handle of a coffee pot, which is not specially designed for this gripper, and it can pour the coffee at the exact location of a cup. The gripper can remove a fluorescent bulb from a socket. This task requires a stable and firm grip to hold the bulb [see Fig. 16(f)]. Fragile objects can be held with a stable grip so that the gripper can perform more complicated tasks that are not only simple pick-and-place operations but more complex tasks requiring a firm and strong grip, such as assembly disassembly operations. The weight of each object is as follows: ripe persimmon (170 g), tomato (130 g), grape (680 g), tofu (360 g), coffee server with coffee (770 g), fluorescent bulb (110 g), paper cup with coffee (220 g), chicken (1130 g), water bottle (2050 g), pot (770 g), cocktail glass (260 g), pan (600 g), and squid (270 g).



Fig. 16. Examples of practical application of the universal soft gripper. (a) Pick and place of a ripe persimmon. (b) Tomato. (c) Grapes, and (d) tofu (Supplementary video 2). (e) Pouring coffee using a server. (f) Removing a fluorescent bulb from a socket. (g) Pouring coffee out from a paper cup (Supplementary video 3). (h) Cooking whole chicken soup. (i) Making a cocktail with a squeezed lemon. (j) Cooking a squid dish (Supplementary video 4).

V. CONCLUSION

In this study, shape-adaptive tips for parallel grippers capable of adapting their contour to a target object in a very soft state and of firmly holding the object in a stiff state were presented. The shape-adaptive tips have very low stiffness until the parallel gripper finishes closing the tips toward target object; therefore, even an extremely soft and/or fragile object can be safely held by using the developed tips. To achieve a very low stiffness tip and a target-matched shape, a soft supporting layer, which consisted of a polymeric honeycomb structure, and two stretchable shape retention layers, which consist of a stretchable sewn mesh structure filled with granular particles, are proposed. In particular, the force required to deform the soft supporting layer does not linearly increase but remains relatively constant during the deformation process, and this effect, which is due to the collapse region of the honeycomb structure, helps minimize the required normal force even when the deformation depth increases. Due to these characteristics of this gripper, the initial stiffness of the gripper before jamming can be similar to that of tofu, so the gripper tip can be safely deformed to match the shape of the gripper target object with very low stiffness. This was difficult to realize in previous research, in which bags that were fully filled with particles were used [19], owing to the relatively high stiffness. After finish closing gripper, the stiffness of the shape retention layers was increased, and a sidewall design was adapted into the shape retention layers to increase the shear modulus of the structure. The gripping performance of the developed shape-adaptive tip when using the parallel gripper was evaluated, and the highest gripping efficiency was

measured as 2.75 for a 50 mm round-shaped object. This value was approximately twice as high as that obtained in previous similar research by Yusuke Tsugami *et al.* [12]. The gripping force of this gripper in the stiff state was only increased by approximately 2.3 compared to that in the soft state, and this value was also lower than that of our proposed gripper, which was 4.0. The developed gripper also offers the advantage that there is no limit to the shape configuration, compared to previous stiffness-changeable grippers with rubber bags that were fully filled with materials with mostly a rounded shape, owing to the pressure distribution or hanging down resulting from the large specific gravity. The developed gripper could safely grip the hard-to-grip objects, such as a ripe persimmon, tofu, and grapes, and even a coffee pot with an irregular handle, as well as a fluorescent bulb, could be controlled to fulfill the required tasks. However, the developed gripper exhibits the limitation whereby the gripping efficiency decreases when the contact surface is flat. In particular, when the size of the flat-shaped object was larger than the area of the shape-adaptive tip, the gripping efficiency decreased to approximately 0.4, which was a similar value to that of the general gripper. This is because the adapted shape of the tip became flat, which was similar to the shape of the tip in the previous general gripper. The other limitation of the developed gripper is the wetting condition; it exhibited an approximately 77% gripping efficiency compared to that in the nonwetting condition for the 50 mm ball-shaped object. However, this decreased gripping efficiency was still much higher than that of the previous general parallel gripper. The other required improvement of the gripper is the autonomous feedback control to adjust the gripping distance. The contact sensor to measure the target depth of deformation of the gripper to decide the gripping distance will be studied in the next research. The developed shape-adaptive soft parallel gripper can become a universal gripper, and it provides a favorable solution using tools readily available in the industry without the need to design specific tools for each target object as the safe solution for the human-robot collaboration process.

REFERENCES

- [1] W. Chung, C. Rhee, Y. Shim, H. Lee, and S. Park, "Door-Opening control of a service robot using the multifingered robot hand," *IEEE Trans. Ind. Electron.*, vol. 56, no. 10, pp. 3975–3984, Oct. 2009.
- [2] T. Mettler, M. Sprenger, and R. Winter, "Service robots in hospitals: New perspectives on niche evolution and technology affordances," *Eur. J. Inf. Syst.*, vol. 26, no. 5, pp. 451–468, Sep. 2017.
- [3] A. D. Dragan, S. Bauman, J. Forlizzi, and S. S. Srinivasa, "Effects of robot motion on human-robot collaboration," in *Proc. ACM/IEEE Int. Conf. Human-Robot Interact.*, Mar. 2–5, 2015, pp. 51–58.
- [4] H. Liu, "Exploring human hand capabilities into embedded multifingered object manipulation," *IEEE Trans. Ind. Informat.*, vol. 7, no. 3, pp. 389–398, Aug. 2011.
- [5] Ottobock, "Bebionic hand Ottobock U.S." 2018. Accessed on: Dec. 21, 2020. [Online]. Available: <https://www.ottobockus.com/prosthetics/upper-limb-prosthetics/solution-overview/bebionic-hand>
- [6] L. B. Bridgwater *et al.*, "The robonaut 2 hand—Designed to do work with tools," in *Proc. IEEE Int. Conf. Robot. Autom.*, Saint Paul, MN, USA, 2012, pp. 3425–3430.
- [7] M. Honarpardaz, M. Tarkian, J. Ivander, and X. Feng, "Finger design automation for industrial robot grippers: A review," *Robot. Auton. Syst.*, vol. 87, pp. 104–119, Jan. 2017.
- [8] A. Wolf, R. Steinmann, and H. Schunk, *Grippers in Motion*. Berlin, Germany: Springer, 2005.
- [9] Parker Hannifin Corporation, "Parallel and Angular Grippers," 2016. Accessed on: Dec. 21, 2020. [Online]. Available: <https://www.parker.com/parkerimages/automation/cat/English/1835cint.pdf>
- [10] Y. T. Choi, C. M. Hartzell, T. Leps, and N. M. Wereley, "Gripping characteristics of an electromagnetically activated magnetorheological fluid-based gripper," *AIP Adv.*, vol. 8, no. 5, May 2018, Art. no. 056701.
- [11] T. Nishida, Y. Okatani, and K. Tadakuma, "Development of universal robot gripper using MR α fluid," *Int. J. Humanoid Robot.*, vol. 13, no. 4, 2016, Art. no. 1650017.
- [12] Y. Tsugami, T. Barbi, K. Tadakuma, and T. Nishida, "Development of universal parallel gripper using reformed magnetorheological fluid," in *Proc. 11th Asian Control Conf.*, 2017, pp. 778–783.
- [13] A. Pettersson, S. Davis, J. O. Gray, T. J. Dodd, and T. Ohlsson, "Design of a magnetorheological robot gripper for handling of delicate food products with varying shapes," *J. Food Eng.*, vol. 98, no. 3, pp. 332–338, 2010.
- [14] J. Shintake, B. Schubert, S. Rosset, H. Shea, and D. Floreano, "Variable stiffness actuator for soft robotics using dielectric elastomer and low-melting-point alloy," in *Proc. IEEE/RSJ Int. Conf. Intell. Robot. Syst.*, Hamburg, Germany, 2015, pp. 1097–1102.
- [15] H. Nakai, Y. Kuniyoshi, M. Inaba, and H. Inoue, "Metamorphic robot made of low melting point alloy," in *Proc. IEEE/RSJ Int. Conf. Intell. Robot. Syst.*, 2002, vol. 2, pp. 2025–2030.
- [16] M. Liu, L. Hao, W. Zhang, and Z. Zhao, "A novel design of shape-memory alloy-based soft robotic gripper with variable stiffness," *Int. J. Adv. Robot. Syst.*, vol. 17, no. 1, 2020, doi: [10.1177/1729881420907813](https://doi.org/10.1177/1729881420907813).
- [17] H. M. Jaeger, "Celebrating soft matter's 10th anniversary: Toward jamming by design," *Soft Matter*, vol. 11, no. 1, pp. 12–27, 2015.
- [18] J. Amend and H. Lipson, "The JamHand: Dexterous manipulation with minimal actuation," *Soft Robot.*, vol. 4, no. 1, pp. 70–80, Mar. 2017.
- [19] E. Brown *et al.*, "Universal robotic gripper based on the jamming of granular material," *Proc. Nat. Acad. Sci. USA.*, vol. 107, no. 44, pp. 18809–18814, Nov. 2010.
- [20] J. Amend, N. Cheng, S. Fakhouri, and B. Culley, "Soft robotics commercialization: Jamming grippers from research to product," *Soft Robot.*, vol. 3, no. 4, pp. 213–222, Dec. 2016.
- [21] Y. Wei *et al.*, "A novel, variable stiffness robotic gripper based on integrated soft actuating and particle jamming," *Soft Robot.*, vol. 3, no. 3, pp. 134–143, Sep. 2016.
- [22] J. Zhou *et al.*, "Adaptive variable stiffness particle phalange for robust and durable robotic grasping," *Soft Robot.*, vol. 7, no. 6, pp. 743–757, Dec. 2020.
- [23] M. Zhu, Y. Mori, T. Wakayama, A. Wada, and S. Kawamura, "A fully multi-material three-dimensional printed soft gripper with variable stiffness for robust grasping," *Soft Robot.*, vol. 6, no. 4, pp. 507–519, 2019.
- [24] Y. Gao, X. Huang, I. S. Mann, and H.-J. Su, "A novel variable stiffness compliant robotic gripper based on layer jamming," *J. Mech. Robot.*, vol. 12, no. 5, p. 051013, Jun. 2020.
- [25] T. Wang, J. Zhang, Y. Li, J. Hong, and M. Y. Wang, "Electrostatic layer jamming variable stiffness for soft robotics," *IEEE/ASME Trans. Mechatronics*, vol. 24, no. 2, pp. 424–433, Apr. 2019.
- [26] V. Kargaudas, N. Adamukaitis, M. muida, A. Pakalnis, and S. Zadrauskas, "Elastic foundation displacement approximations," *Balt. J. Road Bridg. Eng.*, vol. 14, no. 2, pp. 125–135, Jun. 2019.
- [27] A. P. Selvadurai, *Elastic Analysis of Soil-Foundation Interaction*. Amsterdam, The Netherlands: Elsevier, 2013.
- [28] KOSMEK, "High-power parallel gripper," 2017. Accessed on: Dec. 21, 2020. [Online]. Available: <http://www.kosmek.co.jp/data/pdf/en/SBR-WPS001-01-GB.pdf>
- [29] T. Zajac, Zaytran Automation, "Robotic Grippers and Gripper sizing in applications," 2005. Accessed on: Dec. 21, 2020. [Online]. Available: <http://www.grippers.com/size.htm>
- [30] M. Kundu, S. Pal, S. Bhui, B. Hansda, and S. Das, "On the use of flexible materials for robot gripping application," *J. Assoc. Eng. India.*, vol. 84, no. 3, pp. 79–85, 2014.



Jae-Young Lee received the M.S. degree in mechanical engineering from Chungnam national University, Daejeon, South Korea, in 2019. He is currently working toward the Ph.D. degree in mechanical engineering with Sungkyunkwan University, Suwon, South Korea.

Since 2017, he has been with the Department of Robotics and Mechatronics, Korea Institute of Machinery and Materials, Daejeon. His research interests include soft robotics and soft mechanism.



Yong-Sin Seo received the M.S. degree in mechanical engineering from Chungnam National University, Daejeon, South Korea, in 2019.

He is currently a Student Researcher with the Department of Robotics and Mechatronics, Korea Institute of Machinery and Materials, Daejeon. His research interests include human-mimetic robot manipulator and soft pneumatic gripper for collaborative robot.



Jongwoo Park received the M.S. and Ph.D. degrees in control and instrumentation engineering from Korea University, Seoul, South Korea, in 2007 and 2016, respectively.

He is currently a Senior Researcher with the Department of Robotics and Mechatronics, Korea Institute Machinery and Materials (KIMM), Daejeon, South Korea. His research interests include analysis of robot control, integrative system for robot, human hand motion, and its synthesis for engineering purposes.



Chanhun Park received the B.S. degree in mechanical engineering from Yeungnam University, Gyeongsan, South Korea, the M.S. degree in mechanical engineering from POSTECH, Pohang, South Korea, and the Ph.D. degree in mechanical engineering from KAIST, Daejeon, South Korea, in 1994, 1996, and 2010, respectively.

Since 1996, he has been a Principal Researcher with the Department of Robotics and Mechatronics, Korea Institute of Machinery and

Materials, Daejeon. Since 2017, he has been a Head of Department of Robotics and Mechatronics, Korea Institute of Machinery and Materials. His research interests include robot manipulator design and control, force-feedback control system, cooperative robot and its application, dexterous manipulators for industrial robotics, gripper systems for human-robot cooperation, and assembly process automation.



Hugo Rodrigue (Member, IEEE) was born in Montreal, QC, Canada, in 1985. He received the B.Eng. degree in mechanical engineering from McGill University, Montreal, in 2008, the M.S. degree in industrial engineering from the Ecole Polytechnique de Montreal, Montreal, QC, Canada, in 2010, and the Ph.D. degree in mechanical and aerospace engineering from Seoul National University, Seoul, South Korea, in 2015.

He is currently an Assistant Professor with the School of Mechanical Engineering, Sungkyunkwan University, Seoul. His research interests are soft actuation, smart materials, and soft robotics.



Je-Sung Koh (Member, IEEE) received the B.S. and Ph.D. degrees in mechanical and aerospace engineering from Seoul National University, Seoul, South Korea, in 2008 and 2014, respectively.

He was a Postdoctoral Fellow with the Harvard Microrobotics Laboratory until 2017. He is currently an Assistant Professor in Mechanical Engineering with the Aju University, Suwon, South Korea. His research interests include biologically inspired, small-scale robot design, and soft robots.



Byeungin Kim received the Ph.D. degree in mechanical engineering from Chungnam University, Daejeon, South Korea, in 2012.

He is currently a Managerial Researcher with the Department of Robotics and Mechatronics, Korea Institute Machinery and Materials (KIMM), Daejeon. His research interests include advanced manufacturing systems, industrial robot system, robot gripper, and precision machinery.



Uikyum Kim (Member, IEEE) received the B.S. and Ph.D. degrees in mechanical engineering from Sungkyunkwan University, Suwon, South Korea, in 2011 and 2017, respectively.

Since 2017, he has been a Senior Researcher with the Department of Robotics and Mechatronics, Korea Institute of Machinery and Materials, Daejeon, South Korea. His research interests include robot hand, surgical robot, six-axis force/torque sensor, force/tactile sensors for robotics applications, haptic interfaces, force-

feedback control system, dexterous manipulators for industrial robotics, soft sensor, and sensor calibration computing algorithms.



Sung-Hyuk Song received the B.S. degree in physics from Korea University, Seoul, South Korea, in 2011, and the Ph.D. degree in mechanical and aerospace engineering from Seoul National University, Seoul, in 2016.

He was a Research Fellow in Regenerative Medicine with the Wake Forest Baptist Medical Center, Winston-Salem, NC, USA, in 2016. Since 2017, he has been a Senior Researcher with the Department of Robotics and Mechatronics, Korea Institute of Machinery and

Materials, Daejeon, South Korea. His research interests include soft robotics, soft morphing structure, 3-D printing in manufacturing, cooperative robot and its application, multipurpose end effector for industrial field, wearable robot, artificial muscle, manufacturing automation, personal mobility, and induction heating process using soft material.